

Article

Fabrication of Photocatalyst Composite Coatings of Cr-TiO₂ by Mechanical Coating Technique and Oxidation Process

Sujun Guan ¹, Liang Hao ², Yun Lu ^{3,*}, Hiroyuki Yoshida ⁴ and Hiroshi Asanuma ³

¹ Graduate School, Chiba University, 1-33, Yayoi-cho, Inage-ku, Chiba 263-8522, Japan; E-Mail: guansujun1222@gmail.com

² College of Mechanical Engineering, Tianjin University of Science and Technology, No.1038, Dagu Nanlu, Hexi District, Tianjin 300222, China; E-Mail: haoliang@tust.edu.cn

³ Graduate School & Faculty of Engineering, Chiba University, 1-33, Yayoi-cho, Inage-ku, Chiba 263-8522, Japan; E-Mail: asanuma@faculty.chiba-u.jp

⁴ Chiba Industrial Technology Research Institute, 6-13-1, Tendai, Inage-ku, Chiba 263-0016, Japan; E-Mail: h.yshd14@pref.chiba.lg.jp

* Author to whom correspondence should be addressed; E-Mail: luyun@faculty.chiba-u.jp; Tel.: +81-43-290-3514; Fax: +81-43-290-3039.

Academic Editor: Joaquim Carneiro

Received: 4 August 2015 / Accepted: 10 September 2015 / Published: 11 September 2015

Abstract: The photocatalyst composite coatings on alumina (Al₂O₃) balls had been prepared by mechanical coating technique (MCT) with titanium (Ti) powder, adding a certain content of chromium (Cr) powder and a subsequent oxidation process. The effect of oxidation conditions and adding Cr on the composite coatings of chromium-titanium dioxide (Cr-TiO₂) was investigated. The results show Cr-TiO₂ coatings are with mixed-phase of anatase and rutile under different oxidation conditions, and the mass fraction of the rutile phase (X_R) has been obviously increased when under 973 K. The SEM images indicate that adding Cr could significantly accelerate the growth of surface structures, especially at 1073 K. The photocatalytic activity of Cr-TiO₂ coatings firstly increases, then decreases, with the addition of Cr. Compared with that of two other oxidation conditions, the enhancement on photocatalytic activity by adding Cr under visible light is relatively higher, especially at 973 K for 10 h.

Keywords: Cr-TiO₂; composite coatings; oxidation condition; mixed-phase; phase transformation

1. Introduction

TiO₂ has been considered as one of the most promising photocatalysts for the potential material in environment purification, sterilization, self-cleaning surfaces, and hydrogen generation due to its high photocatalytic activity, excellent chemical stability, non-toxicity, and low cost [1–3]. However, the photoreaction efficiency of TiO₂ is severely limited to its wider band gap (>3 eV) capable of absorbing only UV radiation [4–6]. Therefore, much effort has been devoted to shifting the absorption of TiO₂ from UV to the visible light range. Cr has attracted numerous attention emerging significant characteristics as an acceptor dopant in the band gap to absorb the photons of the solar spectrum, which allows photons with some lower energy and exhibit a higher photocatalytic activity under visible light [7–10]. Choudhury *et al.* reported the absorption of TiO₂ doped with different amounts of Cr shifted to the visible region due to the substantially-narrowed band gap [9]. In addition, the photocatalytic activity of metal oxide-TiO₂ catalysts is another way for the purpose of improving TiO₂ photocatalytic activity, by increasing the charge separation and extending the energy range of photoexcitation [10].

On the other hand, the mixed-phase is another way to increase the charge transfer of electrons and holes between the phases of anatase and rutile, to which much attention has been paid [11–14]. Yan *et al.* synthesized the TiO₂ with different content of anatase and studied the relationship between photocatalytic activity and synergistic effect of anatase and rutile [11]. He *et al.* fabricated the TiO₂ with the 3D flower-like structure containing different ratio of anatase and rutile, and found the photocatalytic activity show best, when the ratio is 80:20 [12].

In this work, photocatalyst composite coatings of Cr-TiO₂ were prepared by MCT with Ti powder adding a certain content of Cr powder and subsequent oxidation process. The crystal structure and microstructure of the photocatalyst composite coatings were investigated. The effect of oxidation conditions on crystal structure and photocatalytic activity under UV and visible light was examined and discussed.

2. Experimental

2.1. Fabrication

Ti powder (purity of 99.1%, average diameter of 30 μm, Osaka Titanium technologies, Kishiwada, Japan) and Cr powder (purity of 98.0%, average diameter of 10 μm, Nilaco, Tokyo, Japan) were used as the coating materials. Al₂O₃ balls (purity of 93.0%, average diameter of 1 mm, Nikkato, Sakai, Japan) were used as the substrates. A planetary ball mill (Type: P6, Fritsch, Idar-Oberstein, Germany) was employed to perform the mechanical coating operation. The rotation speed of the planetary ball mill was set at 480 rpm for 10 h with a 10-min milling operation and a following 2 min cooling interval to prevent the bowl from overheating. After the operation of MCT, the composite coatings on Al₂O₃ balls were oxidized at the temperatures of 1073 K for 3 h, and 973 K for 3 and 10 h, using an electric furnace in air, then cooled to room temperature in the furnace [15].

2.2. Characterization

The prepared samples were labeled as follows. “M10- x Cr” indicates that the samples prepared by mixed Ti and Cr powder, with x being the mass fraction of Cr by MCT at 480 rpm for 10 h. “M10- x Cr- y K/ z h” are the oxidized samples of “M10- x Cr”, oxidation at the temperature of y K for z h. X-ray diffraction (XRD, JDX-3530, JEOL, Tokyo, Japan) with Cu- $K\alpha$ radiation at 30 kV and 20 mA was used to determine the compositions and crystal structures. The surface morphologies and cross-sectional microstructures of the samples were observed by scanning electron microscopy (SEM, JSM-5300, JEOL, Tokyo, Japan). Ultraviolet-visible (UV-VIS) absorption spectra of the M10- x Cr-973 K/10 h samples was measured by a UV-VIS spectrophotometer (MSV-370, JASCO, Tokyo, Japan) with a wavelength range of 370–700 nm.

2.3. Photocatalytic Activity

Evaluation method of photocatalytic activity was referenced to Japanese industrial standard (JIS R 1703-2 2014). First, the prepared samples firstly dried under UV light (FL20S BLB, Toshiba, Tokyo, Japan) for 24 h, and adsorption of methylene blue (MB) solution (20 $\mu\text{mol/L}$, 35 mL) was carried out in the dark for 18 h. After these treatments, the photocatalytic activity was evaluated by measuring the degradation rate of MB solution (C_0 : 10 $\mu\text{mol/L}$, 35 mL) at room temperature. The photocatalytic activity test under UV had been detail reported in our previous work [15]. On the other hand, the photocatalytic activity test under visible light was carried out by the light source (irradiance of 5000 lux) with two 20 W fluorescent lamps (NEC FL20SSW/18). A suitable cut-off filter (L42, Hoya Candeo Optronics Co., Toda, Japan) was used to ensure that only visible light ($\lambda > 420$ nm) could reach the samples. The degradation rate constant k ($\text{nmol}\cdot\text{L}^{-1}\cdot\text{min}^{-1}$) of MB solution concentration *versus* irradiation time was calculated by the least squares method with the data. In order to clearly show the photocatalytic activity of samples, here use R value to describe the difference of the degradation rate constants k . R is calculated by this equation:

$$R = k_{\text{sample}} - k_{\text{MB}} \quad (1)$$

where k_{MB} is to describe the degradation rate constants of MB solution without samples.

3. Results and Discussion

3.1. Appearance and Phase Evolution of Photocatalyst Composite Coatings

The M10- x Cr samples show metallic color, which is same to that of Ti coatings [16]. In contrast, the M10- x Cr- y K/ z h samples appear various colors, which are brown to light-black at 973 K for 3 h, and light-blue to yellow at 1073 K for 3 h, then light-black to dark-blue at 973 K for 10 h, as shown in Figure 1. With adding Cr, the color of the samples obviously changes at each oxidation condition. The color change of photocatalyst composite coatings hints that the Cr had effected on the oxygen vacancies, which produces the color centers of Ti^{3+} in the TiO_2 [17,18].

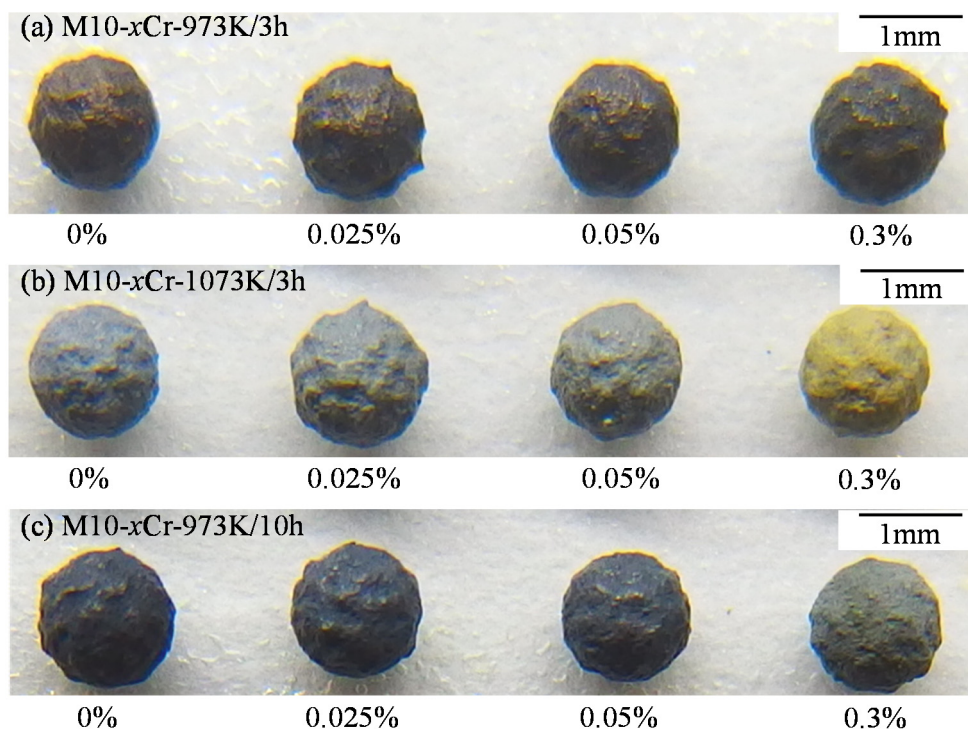


Figure 1. The appearance photograph of the samples. (a) M10-xCr-973 K/3 h; (b) M10-xCr-1073 K/3 h; (c) M10-xCr-973 K/10 h.

Figure 2 shows the XRD patterns of the samples; the diffraction peaks are consistent with the values in the standard card (JCPDS, No. 21-1276 and 89-4921). No characteristic peak of chromium oxide has been found, which hints either doped Cr was incorporated in the crystalline structure of the TiO_2 , or the chromium oxide was highly dispersed and its size was too small to be detected. The same results have been reported by many references [19–21]. The relatively higher diffraction peaks of anatase are detected from the M10-xCr-973 K/3 h, and the peaks of rutile become to be higher, with increasing the oxidation temperature to 1073 K or extending the oxidation time to 10 h. The effect on the phase transformation by adding Cr is relatively slight, along the red lines in Figure 2. The change becomes obvious until the content of Cr reaches 0.3%, as shown in Table 1, which is calculated from the respective peak intensities using the following equation [22]:

$$X_R (\%) = (1 - (1 + 1.26 I_R/I_A)^{-1}) \times 100 \quad (2)$$

where I_R and I_A are X-ray intensities of the rutile (110) and anatase (004) peaks, respectively. The change of X_R is significant, especially at the temperature of 973 K. The phase transformation from anatase to rutile with the present of Cr has been reported by many studies [23–25]. The reason could be considered to be a consequence of the Cr into the TiO_2 lattice. When the low content of Cr substitutes for Ti^{4+} in the TiO_2 , the lattice could keep the crystal structure, thus, the X_R does not change too much with 0.025% and 0.05% of Cr. While the content of Cr up to 0.3%, high content of Cr would cause the formation of more oxygen vacancies, which could accelerate the phase transformation from anatase to rutile to better accommodate the excess of Cr into the TiO_2 lattice [24,25].

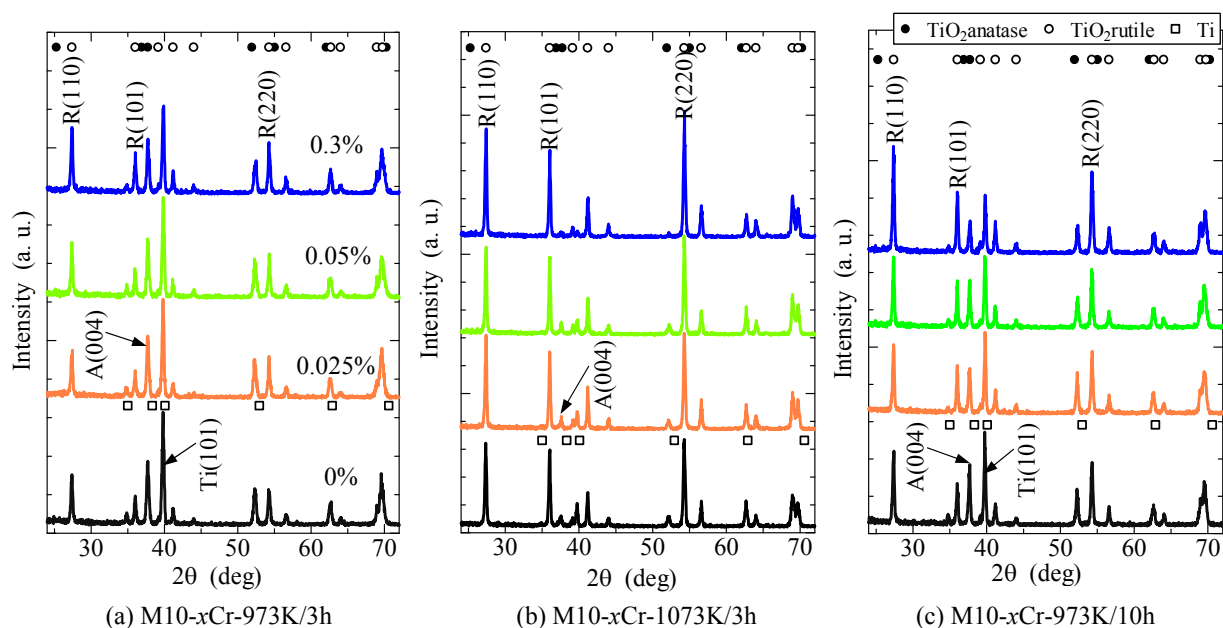


Figure 2. XRD patterns of the samples. (a) M10-*x*Cr-973 K/3 h; (b) M10-*x*Cr-1073 K/3 h; (c) M10-*x*Cr-973 K/10 h.

Table 1. X_R of M10-*x*Cr-*y* K/*z* h samples.

<i>x</i>	<i>y/z</i>		
	973 K/3 h	103 K/3 h	973 K/10 h
0	0.5	0.91	0.6
0.025	0.49	0.9	0.66
0.05	0.54	0.9	0.67
0.3	0.6	0.96	0.8

As far as we know, the phase transformation between anatase and rutile is a metastable-to-stable transformation and the phase transformation temperature range is wide, due to the fabrication process, the shape/size of photocatalyst materials [14,26–28]. When increased the oxidation temperature from 973 K to 1073 K for 3 h, the X_R obviously changes from anatase to rutile; when the oxidation time is extended from 3 h to 10 h at 973 K, the X_R does not change much, compared with increasing the temperature. According to the Gibbs' free energy for the two phases (anatase and rutile), the energy difference ΔG between phase of anatase and rutile at 973 K and 1073 K are about $2761 \text{ J}\cdot\text{mol}^{-1}$ and $2137 \text{ J}\cdot\text{mol}^{-1}$, respectively, calculated by the equations [29], while the effect of extending oxidation time (3 h to 50 h) or adding Cr would accelerate the process of crystal growth or phase transformation [30,31]. Considering these three factors based on the above results, the effect on phase transformation and crystal growth by the oxidation temperature is more direct than that of oxidation time or adding Cr.

3.2. Microstructure Evolution of Photocatalyst Composite Coatings

Figure 3 shows the surface structure evolution of M10-*x*Cr-973 K/3 h samples. With increasing the content of adding Cr, the point-like structure increases in number and grows larger. When increasing the Cr up to 0.3%, the point-like structure significantly grows and almost covers the surface. The evolution

of M10- x Cr-1073 K/3 h samples is shown in Figure 4, compared with increasing the temperature. The microstructure becomes needle-like, and grows to be plate-like along the needle with the increasing content of Cr. When extending the oxidation time to 10 h at 973 K, Figure 5 shows the significant change of surface microstructure, and the size of point-like structures become too large, in the case of adding 0.3% Cr. Considering the changes of surface microstructure and phase transformation, one could draw the conclusion that the phase transformation from anatase to rutile has been effected by the crystal size [31,32]. During each oxidation condition, Cr could accelerate the phase transformation from anatase to rutile, and affect the growth of crystal size, especially at suitable temperature of 973 K [25,30]. However, comprehensive comparison of Figures 3–5, the effect of oxidation temperature on the change of microstructure is more significant than that of oxidation time or the content of adding Cr, as the ΔG is too high at 1073 K.

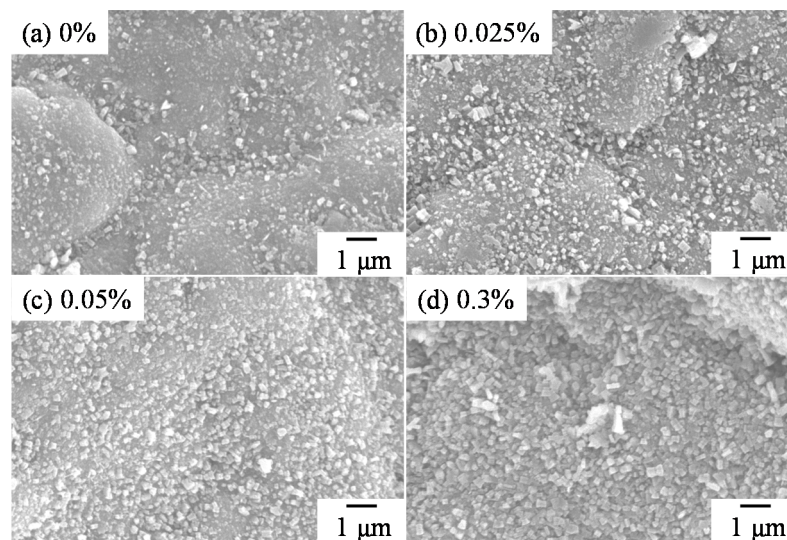


Figure 3. SEM images of surfaces of M10- x Cr-973 K/3 h samples. (a) 0%; (b) 0.025%; (c) 0.05%; (d) 0.3%.

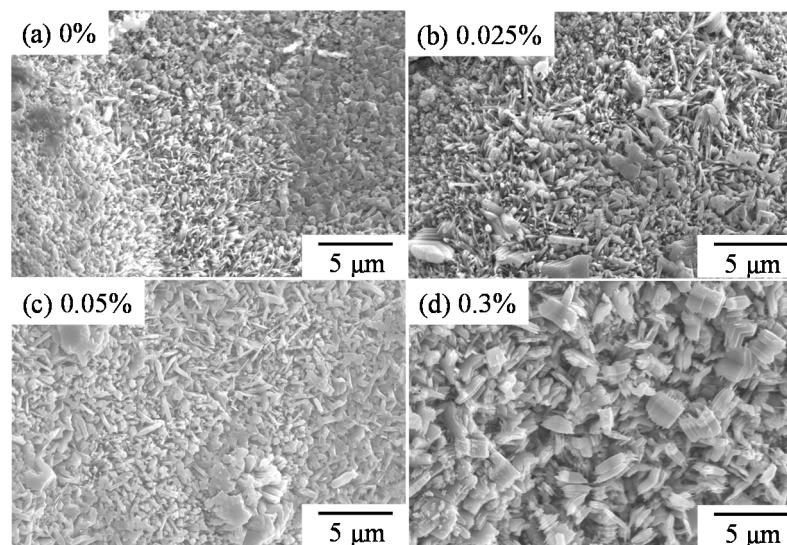


Figure 4. SEM images of surfaces of M10- x Cr-1073 K/3 h samples. (a) 0%; (b) 0.025%; (c) 0.05%; (d) 0.3%.

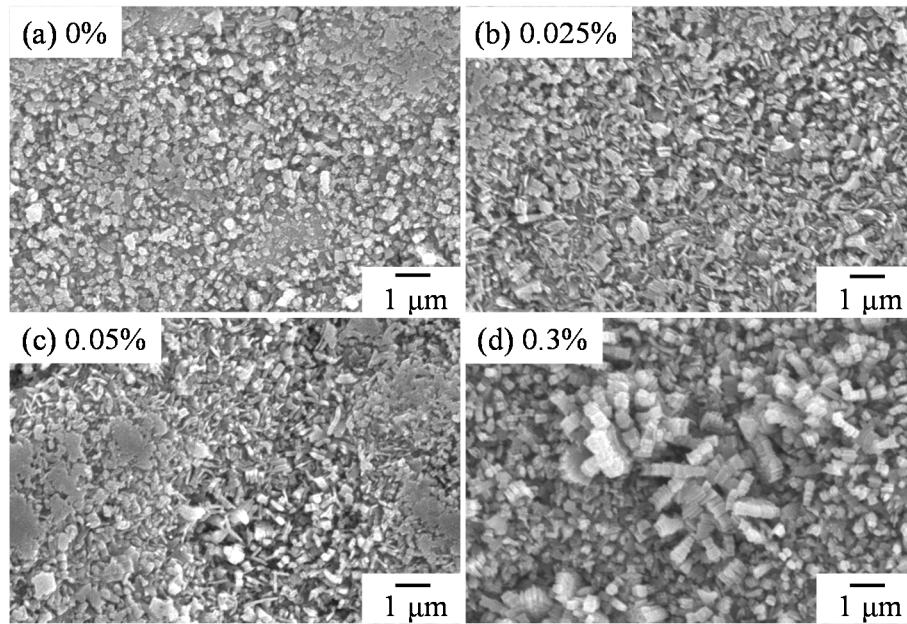


Figure 5. SEM images of surfaces of M10-xCr-973 K/10 h samples. (a) 0%; (b) 0.025%; (c) 0.05%; (d) 0.3%.

Figure 6 shows the cross-sections of the microstructure of M10-xCr-973 K/10 h samples. The oxidized layer grows from about 2 μm (without adding Cr) to be about 5 μm (adding 0.3% Cr), which indicates that the Cr could accelerate the crystal growth, confirmed with the evolution of the surface and cross-section's microstructure.

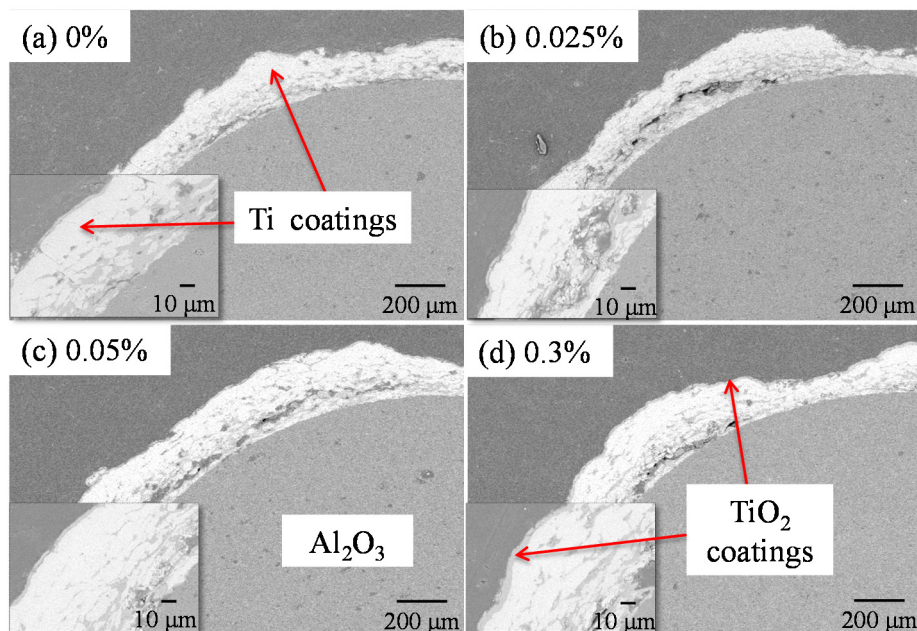


Figure 6. SEM images of cross-sections of M10-xCr-973 K/10 h samples. (a) 0%; (b) 0.025%; (c) 0.05%; (d) 0.3%.

3.3. Photocatalytic Activity of Photocatalyst Composite Coatings

The photocatalytic activity of the samples has been investigated by degradation of MB solution under UV and visible light, as shown in Figure 7. The trend of photocatalytic activity firstly increases and then decreases with adding Cr, under different oxidation conditions. When changing the oxidation temperature (Figure 7b) or the oxidation time (Figure 7c), the photocatalytic activity firstly increases, then decreases, when adding a higher content of Cr. The MB-occupied accessible surface area of TiO₂ coatings is excited to generate hydroxyl radical and superoxide radical that both decomposed the adsorbed MB solution [33,34]. The structurally-defective morphology of Cr-TiO₂ coatings is affected with adding Cr, as reported by references [35,36]. The structurally-defective morphology is an important role to affect the photocatalytic activity of Cr-TiO₂ coatings [37].

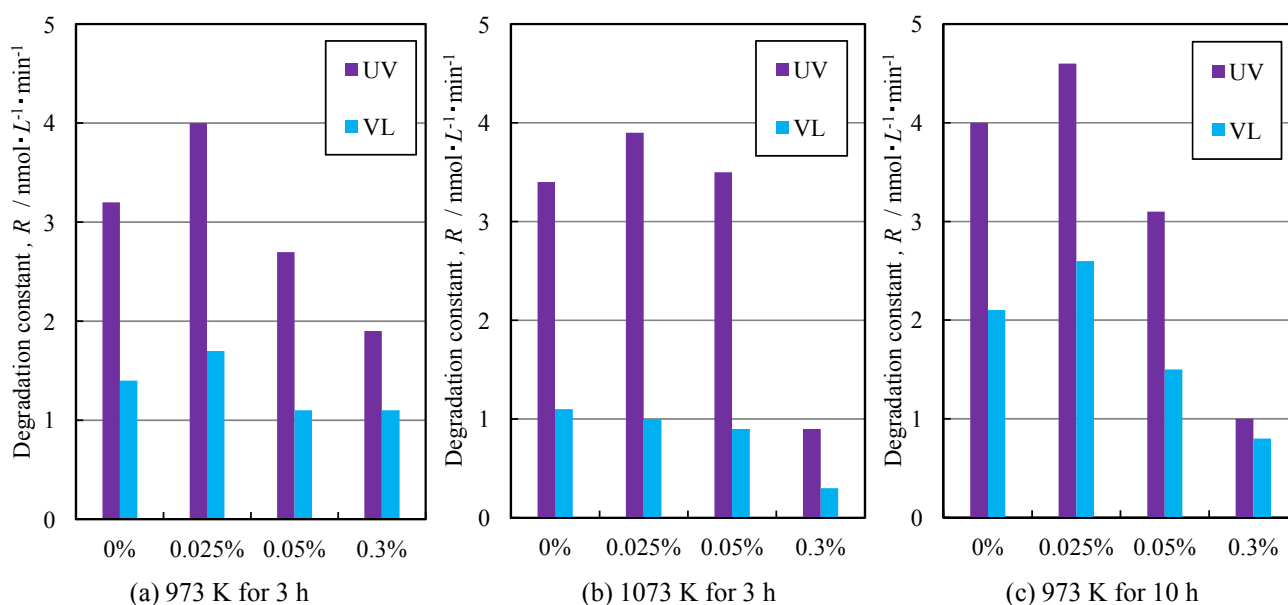


Figure 7. Degradation rate constant of M10-*x*Cr-*y*K samples. (a) 973 K for 3 h; (b) 1073 K for 3 h; (c) 973 K for 10 h.

On the other hand, the mixed-phase of anatase and rutile has a synergistic effect on enhancing the photocatalytic activity of TiO₂ [11,13]. As anatase interweaves with rutile, the electron-hole recombination could be hindered by the charge transfer of electrons and holes between the phases. When X_R is lower, the charge transfer would be limited, as a low content of rutile phase could not effectively enhance the photocatalytic activity [23]. However, too much rutile phase would absorb much of the energy from the light, which would also inhibit the activity, as the photocatalytic activity of rutile phase is lower than that of anatase phase [38–40]. Apart from the synergistic effect of the mixed-phase, another possible reason for the enhancement of photocatalytic activity is that a certain amount of Ti³⁺ surface states or cation vacancies have been formed to maintain the electroneutrality by Cr³⁺ substituting Ti⁴⁺ [41]. Moreover, with higher content of Cr, the excess Cr would be oxidized to form oxide, which would serve as the recombination site to suppress the charge transfer, and the photocatalytic activity shows a substantial decrease, with the addition of 0.3% Cr [42].

The UV-Vis spectra of M10-xCr-973 K/10 h samples in the range of 350–700 nm and their indirect transitions are shown in Figure 8 [11]. With the addition of Cr, the absorption range hardly changes until the content of adding Cr reaches 0.3%, which means that the change of band gap is very small, expect when adding 0.3% Cr. This indicates that Cr powder hardly doped the TiO₂, or the effect on the absorption in the visible region is slight when adding a low content of Cr powder, which is different from being doped with Cr cations. This may relate to the effective doping role of Cr powder being limited. Considering the surface microstructure, the size dependent is another factor to cause this change of band gap [43], especially that the microstructure size becomes larger when adding up to 0.3% Cr.

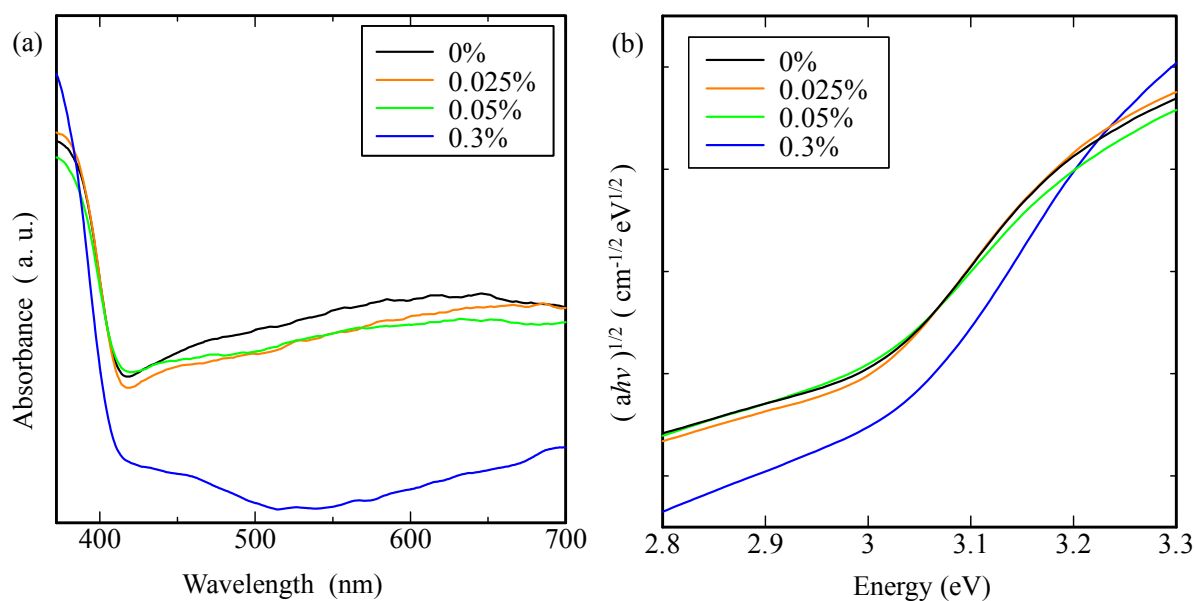


Figure 8. (a) UV-Vis absorption spectra; and (b) the plots of the transformed Kubelka-Munk function *versus* the energy of light over the M10-xCr-973 K/10 h samples.

4. Conclusions

The composite photocatalyst coatings of Cr-TiO₂ have been successfully prepared by MCT and a subsequent oxidation process. The effect of oxidation temperature on phase transformation and crystal growth is more direct than that of oxidation time and adding Cr. With adding Cr, the structure of crystal grows in number and becomes larger, under each oxidation condition. The trend of photocatalytic activity firstly increases and then decreases with adding Cr, under each oxidation condition. It hints at the relationship among photocatalytic activity and the synergistic effect of mixed-phase of anatase and rutile, and compared with that of two other oxidation conditions, the enhancement on photocatalytic activity under visible light is relatively higher at 973 K for 10 h.

Author Contributions

Sujun Guan and Yun Lu conceived and designed the experiments; Sujun Guan performed the experiments; Sujun Guan and Liang Hao analyzed the data; Hiroyuki Yoshida and Hiroshi Asanuma contributed reagents/materials/analysis tools; Sujun Guan wrote the paper.

Conflicts of Interest

The authors declare no conflict of interest.

References

1. Kumar, S.G.; Devi, L.G. Review on modified TiO₂ photocatalysis under UV/visible light: Selected results and related mechanisms on interfacial charge carrier transfer dynamics. *J. Phys. Chem. A* **2011**, *115*, 13211–13241.
2. Nakata, K.; Fujishima, A. TiO₂ photocatalysis: Design and applications. *J. Photochem. Photobiol. C* **2012**, *13*, 169–189.
3. Liu, M.; Qiu, X.; Hashimoto, K.; Miyauchi, M. Cu(II) nanocluster-grafted, Nb-doped TiO₂ as an efficient visible-light-sensitive photocatalyst based on energy-level matching between surface and bulk states. *J. Mater. Chem. A* **2014**, *2*, 13571–13579.
4. Chen, X.; Shen, S.; Guo, L.; Mao, S. Semiconductor-based photocatalytic hydrogen generation. *Chem. Rev.* **2010**, *110*, 6503–6570.
5. Chen, X.; Wang, X.; Hou, Y.; Huang, J.; Wu, L.; Fu, X. The effect of postnitridation annealing on the surface property and photocatalytic performance of N-doped TiO₂ under visible light irradiation. *J. Catal.* **2008**, *255*, 59–67.
6. Asahi, R.; Morikawa, T.; Ohwaki, T.; Aoki, K.; Taga, Y. Visible-light photocatalysis in nitrogen-doped titanium oxides. *Science* **2001**, *293*, 269–271.
7. Akhavan, O. Lasting antibacterial activities of Ag-TiO₂/Ag/a-TiO₂ nanocomposite thin film photocatalysts under solar light irradiation. *J. Colloid Interface Sci.* **2009**, *336*, 117–124.
8. Akhavan, O.; Azimirad, R. Photocatalytic property of Fe₂O₃ nanograin chains coated by TiO₂ nanolayer in visible light irradiation. *Appl. Catal. A Gen.* **2009**, *369*, 77–82.
9. Choudhury, B.; Choudhury, A. Dopant induced changes in structural and optical properties of Cr³⁺ doped TiO₂ nanoparticles. *Mater. Chem. Phys.* **2012**, *132*, 1112–1118.
10. Li, X.; Li, F.; Yang, C.; Ge, W. Photocatalytic activity of WO_x-TiO₂ under visible light irradiation. *J. Photochem. Photobiol. A* **2001**, *141*, 209–217.
11. Yan, M.; Chen, F.; Zhang, J.; Anpo, M. Preparation of controllable crystalline titania and study on the photocatalytic properties. *J. Phys. Chem. B* **2005**, *109*, 8673–8678.
12. He, Z.; Cai, Q.; Fang, H.; Situ, G.; Qiu, J.; Song, S.; Chen, J. Photocatalytic activity of TiO₂ containing anatase nanoparticles and rutile nanoflower structure consisting of nanorods. *J. Environ. Sci.* **2013**, *25*, 2460–2468.
13. Liu, J.; Yu, X.; Liu, Q.; Liu, R.; Shang, X.; Zhang, S.; Li, W.; Zheng, W.; Zhang, G.; Cao, H.; *et al.* Surface-phase junctions of branched TiO₂ nanorod arrays for efficient photoelectrochemical water splitting. *Appl. Catal. B* **2014**, *158–159*, 296–300.
14. Zhang, J.; Xu, Q.; Feng, Z.; Li, M.; Li, C. Importance of the relationship between surface phases and photocatalytic activity of TiO₂. *Angew. Chem. Int. Ed.* **2008**, *47*, 1766–1769.
15. Lu, Y.; Matsuzaka, K.; Hao, L.; Hirakawa, Y.; Yoshida, H.; Pan, F. Photocatalytic activity of TiO₂/Ti composite coatings fabricated by mechanical coating technique and subsequent heat oxidation. *Mater. Sci. Semicond. Process.* **2013**, *16*, 1949–1956.

16. Yoshida, H.; Lu, Y.; Nakayama, H.; Hirohashi, M. Fabrication of TiO₂ film by mechanical coating technique and its photocatalytic activity. *J. Alloys Compd.* **2009**, *475*, 383–386.
17. Hoang, S.; Guo, S.; Hahn, N.; Bard, A.; Mullins, C. Visible light driven photoelectrochemical water oxidation on nitrogen-modified TiO₂ nanowires. *Nano Lett.* **2012**, *12*, 26–32.
18. Lu, X.; Wang, G.; Zhai, T.; Yu, M.; Gan, J.; Tong, Y.; Li, Y. Hydrogenated TiO₂ nanotube arrays for supercapacitors. *Nano Lett.* **2012**, *12*, 1690–1696.
19. Pan, C.; Wu, J. Visible-light response Cr-doped TiO_{2-x}N_x photocatalysts. *Mater. Chem. Phys.* **2006**, *100*, 102–107.
20. Zhu, J.; Deng, Z.; Chen, F.; Zhang, J.; Chen, H.; Anpo, M.; Huang, J.; Zhang, L. Hydrothermal doping method for preparation of Cr³⁺-TiO₂ photocatalysts with concentration gradient distribution of Cr³⁺. *Appl. Catal. B* **2006**, *62*, 329–335.
21. Droubay, T.; Heald, S.; Shutthanandan, V.; Thevuthasan, S.; Chambers, S.; Osterwalder, J. Cr-doped TiO₂ anatase: A ferromagnetic insulator. *J. Appl. Phys.* **2005**, *97*, doi:10.1063/1.1846158.
22. Spuur, R.; Myers, H. Quantitative analysis of anatase-rutile mixtures with an X-ray diffractometer. *Anal. Chem.* **1957**, *29*, 760–762.
23. Hajjaji, A.; Gaidi, M.; Bessais, B.; Khakani, M. Effect of Cr incorporation on the structural and optoelectronic properties of TiO₂:Cr deposited by means of a magnetron co-sputtering process. *Appl. Surface Sci.* **2011**, *257*, 10351–10357.
24. Carp, O.; Huisman, C.L.; Reller, A. Photoinduced reactivity of titanium dioxide. *Prog. Solid State Chem.* **2004**, *32*, 33–177.
25. Gennari, F.C.; Pasquevich, D.M. Enhancing effect of iron chlorides on the anatase-rutile transition in titanium dioxide. *J. Am. Chem. Soc.* **1999**, *82*, 1915–1921.
26. Zhang, X.; Lei, L. One step preparation of visible-light responsive Fe-TiO₂ coating photocatalysts by MOCVD. *Mater. Lett.* **2008**, *62*, 895–897.
27. Verma, R.; Samdarshi, S.K. Correlating oxygen vacancies and phase ratio/interface with efficient photocatalytic activity in mixed phase TiO₂. *J. Alloys Compd.* **2015**, *629*, 105–112.
28. Atitar, M.F.; Ismail, A.A.; Al-Sayari, S.A.; Bahnemann, D.; Afanasev, D.; Emeline, A.V. Mesoporous TiO₂ nanocrystals as efficient photocatalysts: Impact of calcination temperature and phase transformation on photocatalytic performance. *Chem. Eng. J.* **2015**, *264*, 417–424.
29. Liao, S.; Mayo, W.; Pae, K. Theory of high pressure/low temperature sintering of bulk nanocrystalline TiO₂. *Acta. Mater.* **1997**, *45*, 4027–4040.
30. Lu, Y.; Kobayashi, K.; Guan, S.; Hao, L.; Yoshida, H.; Asanuma, H.; Chen, J. Influence of oxidation process on photocatalytic activity of photocatalyst coatings by mechanical coating technique. *Mater. Sci. Semicond. Process.* **2015**, *30*, 128–134.
31. Zhang, H.; Banfield, J.F. Understanding polymorphic phase transformation behavior during growth of nanocrystalline aggregates: Insights from TiO₂. *J. Phys. Chem. B* **2000**, *104*, 3481–3487.
32. Zhang, J.; Xu, Q.; Li, M.; Feng, Z.; Li, C. UV Raman spectroscopic study on TiO₂. II. Effect of nanoparticle size on the outer/inner phase transformation. *J. Phys. Chem. C* **2009**, *113*, 1698–1704.
33. Wu, C.; Chern, J. Kinetics of photocatalytic decomposition of methylene blue. *Ind. Eng. Chem. Res.* **2006**, *45*, 6450–6457.

34. Habibi, M.; Hassanzadeh, A.; Mahdavi, S. The effect of operational parameters on the photocatalytic degradation of three textile azo dyes in aqueous TiO₂ suspensions. *J. Photochem. Photobiol. A* **2005**, *172*, 89–96.
35. Wang, Y.; Liu, H.; Li, Z.; Zhang, X.; Zheng, R.; Ringer, S. Role of structural defects on ferromagnetism in amorphous Cr-doped TiO₂ films. *Appl. Phys. Lett.* **2006**, *89*, doi:10.1063/1.2240139.
36. Bryan, J.; Santangelo, S.; Keveren, S.; Gamelin, D. Activation of high-T_c ferromagnetism in Co²⁺:TiO₂ and Cr³⁺:TiO₂ nanorods and nanocrystals by grain boundary defects. *J. Am. Chem. Soc.* **2005**, *127*, 15568–15574.
37. Yin, J.; Zhao, X. Enhanced electrorheological activity of mesoporous Cr-doped TiO₂ from activated pore wall and high surface area. *J. Phys. Chem. B* **2006**, *110*, 12916–12925.
38. Liu, L.; Zhao, H.; Andino, J.M.; Li, Y. Photocatalytic CO₂ reduction with H₂O on TiO₂ nanocrystals: Comparison of anatase, rutile, and brookite polymorphs and exploration of surface chemistry. *ACS Catal.* **2012**, *2*, 1817–1828.
39. Luttrell, T.; Halpegamage, S.; Tao, J.; Kramer, A.; Sutter, E.; Batzill, M. Why is anatase a better photocatalyst than rutile?—Model studies on epitaxial TiO₂ films. *Sci. Rep.* **2014**, *4*, 1–8.
40. Ozawa, K.; Emori, M.; Yamamoto, S.; Yukawa, R.; Yamamoto, S.; Hobar, R.; Fujikawa, K.; Sakama, H.; Matsuda, I. Electron-hole recombination time at TiO₂ single-crystal surfaces: Influence of surface band bending. *J. Phys. Chem. Lett.* **2014**, *5*, 1953–1957.
41. Zhang, S.; Chen, Y.; Yu, Y.; Wu, H.; Wang, S.; Zhu, B.; Huang, W.; Wu, S.; Synthesis characterization of Cr-doped TiO₂ nanotubes with high photocatalytic activity. *J. Nanopart. Res.* **2008**, *10*, 871–875.
42. Tsai, C.; Teng, H. Chromium-doped titanium dioxide thin-film photoanodes in visible-light-induced water cleavage. *Appl. Surface Sci.* **2008**, *254*, 4912–4918.
43. Vijayalakshmi, R.; Rajendran, V. Synthesis and characterization of nano-TiO₂ via different methods, Archives. *Appl. Sci. Res.* **2012**, *4*, 1183–1190.

© 2015 by the authors; licensee MDPI, Basel, Switzerland. This article is an open access article distributed under the terms and conditions of the Creative Commons Attribution license (<http://creativecommons.org/licenses/by/4.0/>).